

OPTIMOS-EVE optical design of a very efficient, high-multiplex, large spectral coverage, fiber-fed spectrograph at E-ELT

P. Spanò^{*a}, I. Tosh^b, F. Chemla^c

^aINAF - Osservatorio Astronomico di Brera, V. Bianchi 46, I-23807 Merate, Italy;

^bRutherford Appleton Lab., SSTD – STFC, Didcot Oxon, OX11 0QX, UK;

^cObservatoire de Paris, GEPI, 11 Avenue Marcelin Berthelot, F-92190 Meudon, France

ABSTRACT

OPTIMOS-EVE is a fiber-fed, high-multiplex, high-efficiency, large spectral coverage, spectrograph for EELT covering visible and near-infrared simultaneously. More than 200 seeing-limited objects will be observed at the same time over the full 7 arcmin field of view of the telescope, feeding the spectrograph, asking for very large multiplexing at the spectrograph side. The spectrograph consists of two identical units. Each unit will have two optimized channels to observe both visible and near-infrared wavelengths at the same time, covering from 0.37 to 1.7 micron. To maximize the scientific return, a large simultaneous spectral coverage per exposure was required, up to 1/3 of the central wavelength. Moreover, different spectral resolution modes, spanning from 5'000 to 30'000, were defined to match very different sky targets. Many different optical solutions were generated during the initial study phase in order to select that one that will maximize performances within given constraints (mass, space, cost). Here we present the results of this study, with special attention to the baseline design. Efforts were done to keep size of the optical components well within present state-of-the-art technologies. For example, large glass blank sizes were limited to ~35 cm maximum diameter. VPH gratings were selected as dispersers, to improve efficiency, following their superblaze curve. This led to scanning gratings and cameras. Optical design will be described, together with expected performances.

Keywords: High-resolution spectrograph, volume-phase holographic grating, E-ELT instrumentation, multi-object spectrograph

1. INTRODUCTION

The OPTIMOS-EVE combined UV/VIS/NIR spectrograph will be a fibre-fed, medium- to high-resolution spectrograph, with a very large spectral coverage per exposure and a multiplexing factor matched to the very large number of fibres to be projected onto its detector. Many alternatives have been studied, with different layouts and dispersing elements, in order to explore in detail the parameter space, and optimizing performances, while minimizing unit cost.

1.1 Baseline Design

The design of the spectrographs faces a number of particular challenges, in particular the size of the beams coupled with the desire to achieve medium to high spectral resolutions, the very large number of input fibres, the fact that the visual and near-infrared are to be combined into one instrument and the desire for high overall efficiency. To limit the size of the optics required and to still achieve the high spectral resolutions, image slicing at the focal plane with fibre bundles has been adopted^{1,2}. After this basic choice two options have been studied: a smaller spectrograph, with high angle gratings, or a larger spectrograph with smaller angles. Of course, in order to cope with the high number of fibres, the former will be replicated many more times than the latter one.

Based on a trade-off which was a mix of meeting the top level requirements, cost, efficiency, mass, volume, modularity, technical risks and whether the components could be manufactured at all, a choice was made for a large spectrograph with smaller angles. To meet the number of fibres that need to be accommodated two identical copies of the spectrograph are required. Each spectrograph consists of two arms: one covering the visual regime (0.37 – 0.93 μm) and one covering the near-infrared regime (0.93 – 1.7 μm).

*paolo.spano@brera.inaf.it; phone +39 039 5971 063; fax +39 039 5971 001; www.brera.inaf.it/utenti/spano

1.2 Design choices

Optical beam sizes are mainly limited by disperser maximum available size and large glass blanks to make the dioptric cameras. For example, CaF₂ blanks are currently available up to 350mm, mainly produced for lithography applications³.

VPH (volume phase holographic) gratings are chosen for their very large efficiencies, high line densities and low scattered light. Devices up to 40x40cm have been prototyped in the past^{4,5} and match with the collimated beam size. Applying a VPH gives the possibility of a more compact opto-mechanical design, reduce camera size due to smaller distances between dispersers and camera optics. The main disadvantage is represented by more mechanisms for e.g. an articulated camera.

The whole spectrograph system will be mounted in a thermally controlled enclosure filled with dry air and atmospheric pressure for improved stability. For background suppression the temperature is reduced to 193 K. The thermal stability is required to obtain the required level of stability between many different observing modes.

1.3 Overall spectrograph design

One of the two spectrograph units are shown in Figure 1. Light from fibre bundles is split into a UV-VIS beam and a NIR beam by a dichroic. Both channels share the same optical layout and have been optimized for the different wavelengths. Light is collimated by a mirror and two corrector lenses, passes through an order-sorting filter to select the desired wavelengths, and is finally dispersed by VPH gratings. Dispersed beams are focused on the detectors using fast F/1.8 cameras.

The VIS detector-mosaic is enclosed in a cryostat cooled to 173K. The NIR camera including detectors-mosaic is enclosed in a cryostat cooled down to 130 K. Both cryostats are continuous flow nitrogen ones. The whole spectrograph assembly is enclosed in an atmospheric (dry air) cold chamber (refrigerator), cooling the full assembly down to 193 K for H-band background suppression and thermal stability. The two spectrograph units share the same enclosure.

The cold chamber is filled with dry air, cooled by a commercial chiller and dryer. Several panels can be opened to enter the cold chamber for minor interventions. The small holes at the bottom of the wall at the right are cable and pipe throughputs. The optical fibres are fed into the spectrographs via the hood. The hood-throughput is located close to the rotation axis of the positioner⁶. Cabinets for electronics and chiller and dryer are located near the insulating walls. The total projected floor area is within 6x6 m, the blue platform project area is 6x5 m².

Five different observing modes have been defined. Three of them will be dedicated to single point-source, seeing-limited objects, through so-called Mono-Object (MO) buttons, observed at three different spectral resolutions (6000, 18000, 30000). Other two observing modes will provide integral-field units on relatively small (1.8"x3", Medium IFU, or MI) or large (8"x14", Large IFU, or LI) apertures on the sky coupled to low-resolving power.

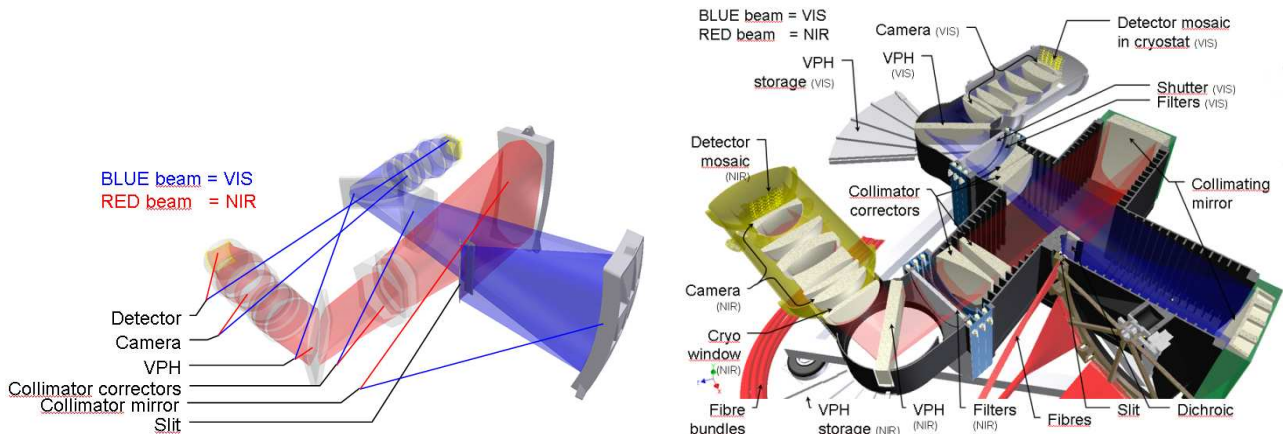


Figure 1. Spectrograph optical layout (left) and its mechanical implementation (right).

2. OPTICAL DESIGN

The optical layout of the combined VIS-NIR spectrograph unit is shown in Figure 2. Both channels share a very similar optical layout, based onto a large spherical collimator mirror working together with two off-axis nearly-achromatic corrector lenses, optimized per each channel, a set of different VPH gratings, optimized to cover the whole spectral range at different spectral resolutions, and fully dioptric cameras. Very large well-corrected flat focal planes (18x18 cm) have been designed to match both a large simultaneous spectral coverage per exposure and a high multiplexing gain.

To cope with very different spectral resolving powers, ranging from $R \sim 5,000$ to $R \sim 40,000$, while keeping multiplexing high with a limited number of different fiber cores, required to use different dispersion elements, characterized with high efficiency, very high line densities and easy interchangeability. VPH gratings fulfill those requirements, if camera optics can be rotated following the optical beam, as shown in Figure 3.

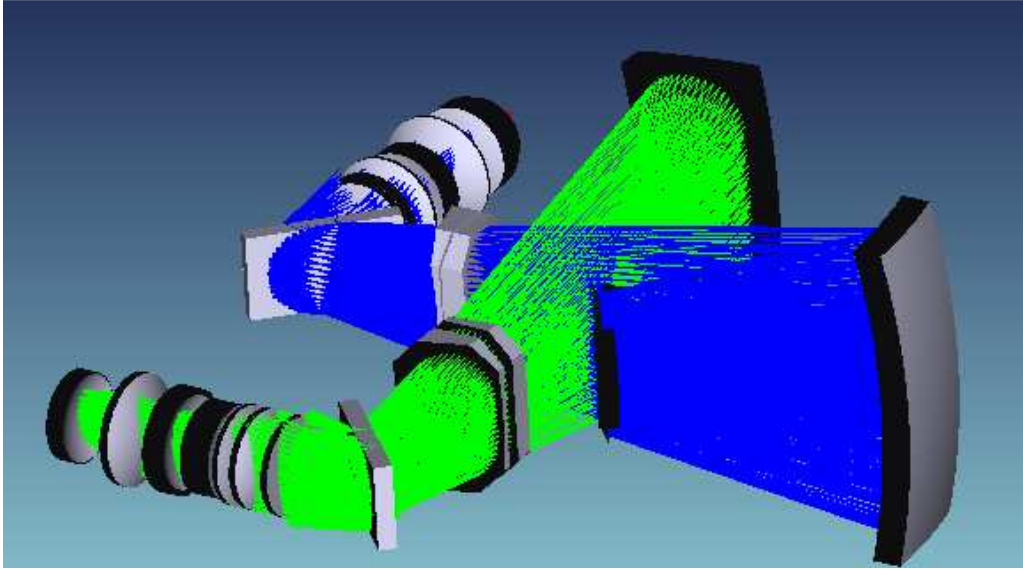


Figure 2. Layout of both VIS (blue) and NIR (green) spectrograph channels.

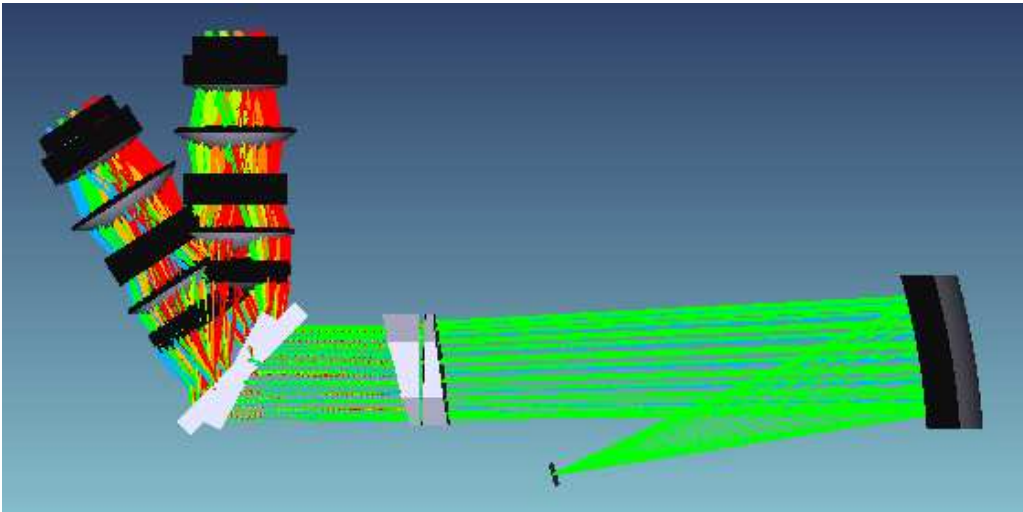


Figure 3. Layout of VIS channel at LR mode (low incidence angle) and HR mode (large incidence angle).

Table 1. Main spectrograph parameters in the different observing modes.

Fiber Button	Low Resolution Modes MO-LR / MI / LI	Medium Res. Mode MO-MR	High Res. Mode MO-HR
Spectral Resolution	6'000	15'000-23'000	26'000-38'000
Wavelength Range	365-930 nm (VIS) 930-1700 nm (NIR)	365-930 nm (VIS) 930-1700 nm (NIR)	365-930 nm (VIS) 930-1700 nm (NIR)
Aperture on sky bundle	0.9 arcsec	0.9 arcsec	0.81 arcsec
Microlens sampling	0.3 arcsec	0.18 arcsec	0.09 arcsec
Sampling of single fibre	>4 pixels (rebin 2x)	>4 pixels	~2 pixels
Multiplex	240 / 30 / 1	70	40
Spectral coverage	~ $\lambda/3$ (VIS) ~ $\lambda/10$ (NIR)	~ $\lambda/6$ (VIS) ~ $\lambda/20$ (NIR)	~ $\lambda/6$ (VIS) ~ $\lambda/20$ (NIR)
Average efficiency	26%	22%	11%
Detector area (VIS)	12kx12k, 15 μ m pixels	12kx12k, 15 μ m pixels	12kx12k, 15 μ m pixels
(NIR)	4kx12k, 15 μ m pixels	4kx12k, 15 μ m pixels	4kx12k, 15 μ m pixels

2.1 First-order parameters

The main system parameters are summarized in Table 1. Then, first-order parameters to design spectrograph sub-systems have been derived to match technical requirements:

- Maximum collimated beam diameter: 28 cm
- Collimator focal ratio: F/3.5 (to match fiber without microlenses)
- Entrance slit length: 33 cm
- Grating incidence angles: 30 deg (LR), 45 deg (MR/HR)
- Camera focal ratio: F/1.8
- Camera field of view: 29 deg

2.2 Entrance area

One of the main goal was to make the entrance aperture as large as possible, to maximize the multiplexing gain of each spectrograph unit and reduce the number of spectrograph units. Moreover, the entrance slit is curved to minimize collimator aberrations. To reduce the size of the dichroic, it has been put as near as possible to the entrance slit. Dichroic is 80x460 mm² large and 20 mm thick, made on a Silica substrate. A flat folding mirror has been added in the VIS channel to help packaging and keep the incidence angle on the dichroic small, reducing the aberrations for the transmitted beam and maximizing spectral performances (slope and efficiency).

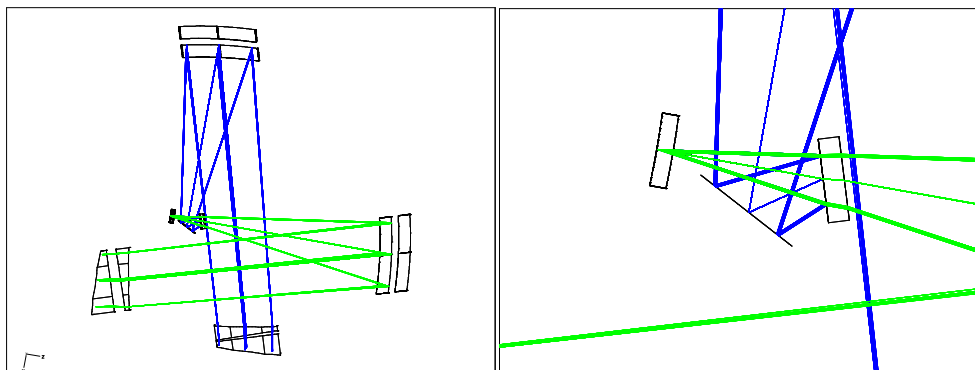


Figure 4. Layout of the collimators (left) and a detailed view of the entrance slit area (right).

Table 2. Gratings installed on each spectrograph, covering both VIS and NIR wavelengths.

Grating	Blaze angle (deg)	Central wavelength (nm)	Bandwidth (nm)	Line density (l/mm)	Observing mode
GR-1-VIS-28-435	28.6	435	365-490	2200	LR
GR-1-VIS-28-580	28.6	580	485-655	1650	LR
GR-1-VIS-28-780	28.6	780	655-875	1230	LR
GR-1-NIR-28-1105	28.6	1105	890-1250	890	LR
GR-1-NIR-28-1490	28.6	1490	1280-1680	660	LR
GR-1-VIS-45-440	41-52	440	365-515	3200	MR/HR
GR-1-VIS-45-590	41-52	590	490-690	2400	MR/HR
GR-1-VIS-45-780	41-52	780	655-915	1800	MR/HR
GR-1-NIR-45-1170	40-50	1170	890-1230	1310	MR/HR
GR-1-NIR-45-1580	41-51	1580	1230-1700	970	MR/HR

2.3 Collimators

After analyzing different collimator designs (full dioptric, all-mirror, or mixed solutions), we selected a Maksutov-type collimator design based onto a single large spherical mirror (about 1m along the largest size), making it cost effective, and two corrector lenses. One of the two correctors is a mild off-axis asphere (4th, 6th, 8th terms added) that can be manufactured directly off-axis. Corrector lenses are about 30x50 cm large. Glasses have been selected to optimized performances and transmission in each channel (BAL15Y/BK7 in the VIS channel, SBSM14/SFPL53 in the NIR). Average efficiency of both collimators is about 90%. Both collimators have been optimized together, because they share the same curved entrance aperture.

Image quality is high enough to match the smallest fibre cores. A relatively large axial chromatism has been left uncorrected, because the camera focal plane is able to refocus for different wavelength regions. The axial chromatism (at the entrance plane) is 2.5 mm in the VIS and 0.4 mm in the NIR. Entrance pupil is positioned not far from the entrance slit, being not telecentric. Moreover, the slit surface is curved. Fibres have been arranged accordingly, to match both chief ray and slit curvature. Figure 5 gives the definition of geometric parameters for a curved slit. Defocus at the edge of each fibre bundle is given by the following formula:

$$RMS(defocus) \approx 0.35 \frac{\delta Z}{F\#} \approx \frac{0.18}{F\#} \frac{lh}{fR} (R - f) \quad (1)$$

2.4 Dispersers

One of the critical choices to build a high-performances spectrograph is the selection of the disperser. Among different types of gratings (surface relief, surface holographic gratings, volume-phase holographic gratings), VPH gratings offer the highest efficiency over a relatively large bandwidth that can be easily tuned over the region of interest. Moreover, VPHs offer additional advantages, like the tunability of the blaze peak changing the incidence angle, low scattered light, and a quite high line density that translates into higher spectral resolution. Finally, they can be produced in large size, up to 28 cm along the groove direction. One of the main goals of OPTIMOS-EVE is to maximize the multi-object spectroscopic performances of EELT, so VPHs can be considered the best choice. A full set of VPHs have been defined to match both resolution and bandwidth of OPTIMOS-EVE, as summarized in Table 2.

VIS and NIR channels will be equipped with 10 different gratings: 5 for LR-modes (3 in the VIS channel and 2 in the NIR one), and 5 MR/HR ones (3 VIS, 2 NIR). In LR mode the required simultaneous spectral coverage is reached without any need to rotate the camera/grating assembly. In MR/HR mode, two exposures per grating are needed to fully cover the whole spectrum, corresponding to two different incidence angles onto the VPH. Also intermediate positions area available to maximize efficiency, following the so-called "superblaze" curve. Each VPH is 28x50 cm² (HR/MR modes) or 28x37 cm² (LR modes). VPH substrates are made in BK7 and 30mm thick. Line densities are within current technology capabilities. Efficiency predictions have been simulated via RCWA, with peak efficiency of 90% (at lower incidence angles) and 75% (at higher incidence angles).

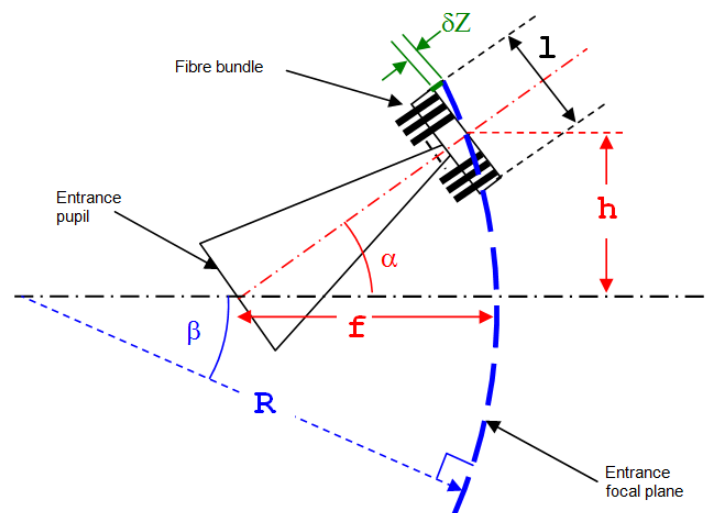


Figure 5. Slit curvature defocus.

Distance from VPH to the camera can be minimized to decrease vignetting and increase image quality. A mechanical solution has been implemented to allow such a mechanism.

Filters to block second order light from VPH are placed in the collimated beam and before the grating. We need only one blocking filter in the VIS channel, with a 0% transmission below 470 nm and a 100% transmission above 640 nm. These quite relaxed requirements make such a filter relatively simple (~20 layers required). It will be inserted only for observing modes looking at the reddest portion of the spectrum. No order sorting filters are required in the NIR channel, except for a blocking filter to prevent any radiation below 850 nm entering the camera. It can be placed on the surface of the camera cryostat.

2.5 Cameras

The VIS and NIR cameras are composed of 7 and 6 lenses respectively, with Schott and Ohara glasses, generally available in large and homogeneous size. Maximum lens diameter is 37 cm. Three mild/strong aspherical surfaces in the VIS camera, and two aspheres in the NIR one, have been added to improve image quality up to the edge of the field of view on a flat focal plane. Axial colours is not corrected, because detector distance and tilt will be actively controlled. Some vignetting has been allowed during the optimization to keep lens diameters below a given value.

Back focal length varies by 4.5 mm to correct for residual axial chromatism of the spectrograph optics. Only two degrees of freedom (piston and tilt) are necessary to refocus and control image quality. Vignetting will vary from a few percent level in LR mode (on average) up to 16% (average) in the worst case. The last lens of the VIS camera is Fused Silica to avoid glass radiation hits onto the CCD. The same was not possible in the NIR camera, to get the best image quality.

NIR camera has a flat Silica entrance window to close the cryostat containing both the camera lenses and the IR array detector assembly.

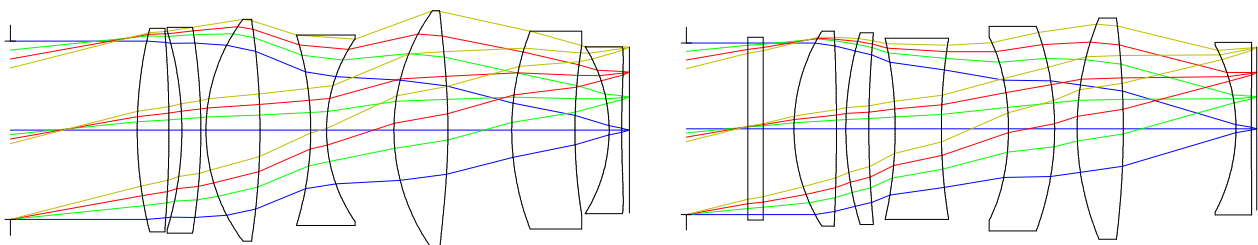


Figure 6. VIS (left) and NIR (right) camera layouts. Entrance aperture is 28 cm in diameter. Focal plane is 18x18 cm.

3. PERFORMANCES

3.1 Image quality

Spectrograph design has been optimized taking into account all different observing modes (e.g., the combination of grating GR-1-VIS-45-440 and a defined incidence angle). Only focal plane refocus and tilt was optimized per each setup. Some spot diagrams for the central wavelength for all the different observing setups and different slit positions are shown in Figure 7. Image quality is getting worse and worse at the extreme wavelengths of each channel. Typical plots of the RMS spot radius (units: μm) for the VIS channel are given in Figure 8.

As a result, many of the observing modes will have an average RMS spot diameter of 2-3 pixels, matching the LR mode (images will be about 8). For MR and HR modes, however, spot size are partially matching the geometric images (5 and 2.5 pixel only, for MR and HR modes, respectively). In that cases, however, the required slit height is smaller than the full available entrance slit and the central field of the slit can be used, where image quality is high enough to convey the highest quality.

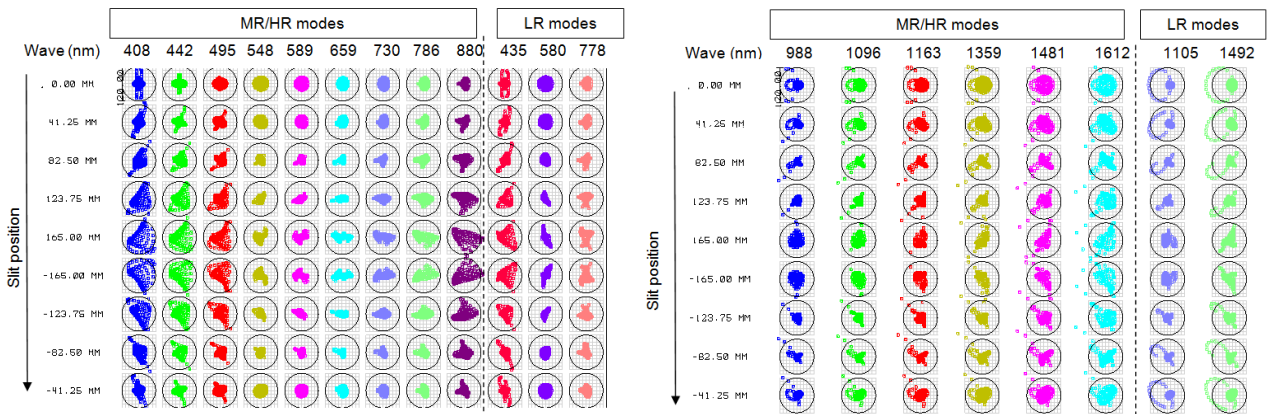


Figure 7. Spectrograph spot diagrams for the VIS arm (left) and NIR arm (right). Different slit position (vertical direction) and different observing setups (horizontal direction), covering both HR (first 9 columns) and LR modes (last 3 columns). Circles represents the image of a LR fibre core. Only central wavelengths are shown.

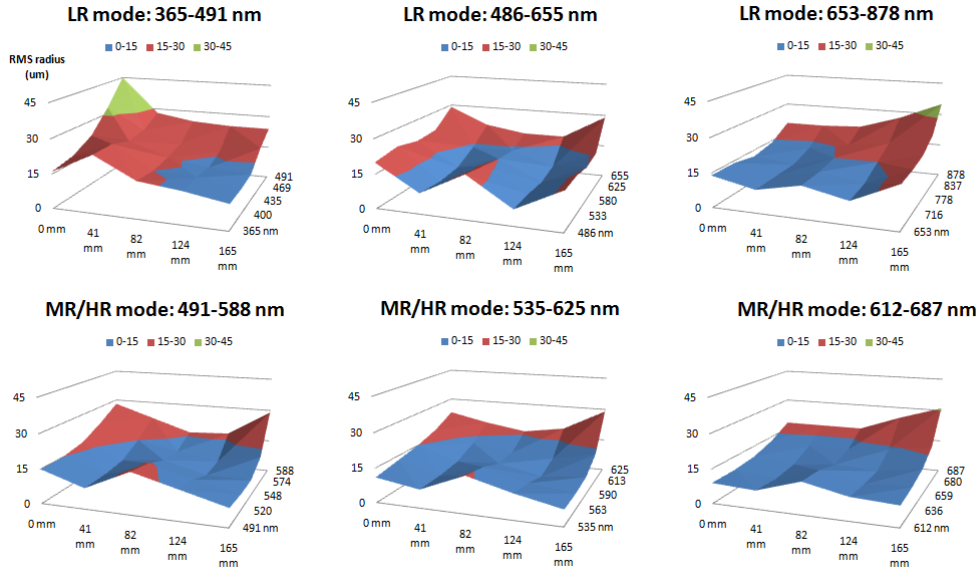


Figure 8. VIS spot radius (μm RMS) vs slit position and wavelength at different observing setups.

3.2 Spectral resolution

Resolving power will depend on the fibre core size the grating incidence angle. Other effects will degrade resolution, like spectrograph image quality, fibre bundle imperfections/defocus, and CCD characteristics (flatness, electro-optical response, sampling). We assume that all these contributions are gaussian noise sources that will add via RSS summation.

In LR mode expected spectral resolution (at blaze peak) is $R=6,000$. In MR mode, $R=18,000$, while in HR mode, $R=30,000$, smaller than expected from pure geometric computation. The largest degradation factor comes from image quality.

3.3 Spectral format

Diffracted orders will be aligned along CCD rows as shown in Figure 9. Different fibres, aligned along the entrance slit, will be projected in the vertical axis of the detector (CCD columns), but a curvature will be present. This effect is larger for the MR/HR modes than for LR ones, due to a higher incidence angle on the grating. This effect can be minimized by introducing a counter-curvature onto the entrance slit, but larger spacing between the slit assembly, the dichroic and the collimator optics is required, not optimized at this stage.

3.4 Efficiency

Efficiency estimate are based onto the following assumptions: air-glass interface 1% loss, 92% efficiency for the large collimator in the VIS (Al coating) and 98% in the NIR (Au coating), a 95% at the dichroic, 2% at the filter (where needed). Internal transmission of glasses has been taken into account. VPH efficiency have been derived from simulation. Vignetting was included as an average efficiency loss at the camera level. A better estimate will properly take into account vignetting only at the edges of spectra.

Figure 10 shows efficiency curves for both LR and MR/HR observing modes, including all factors from the telescope focal plane to the detector focal plane, including detector quantum efficiency.

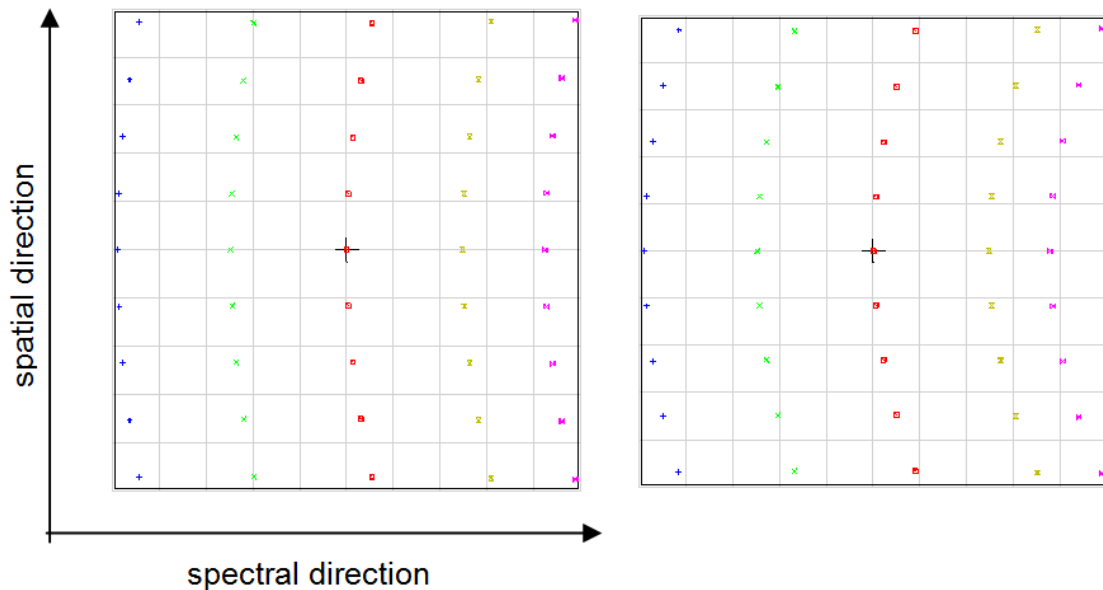


Figure 9. Spectral format for typical LR (left) and MR/HR (right) observing modes. Different colours refer to different wavelengths. Spectra are aligned along the horizontal axis, different fibres will fill the CCD vertically.

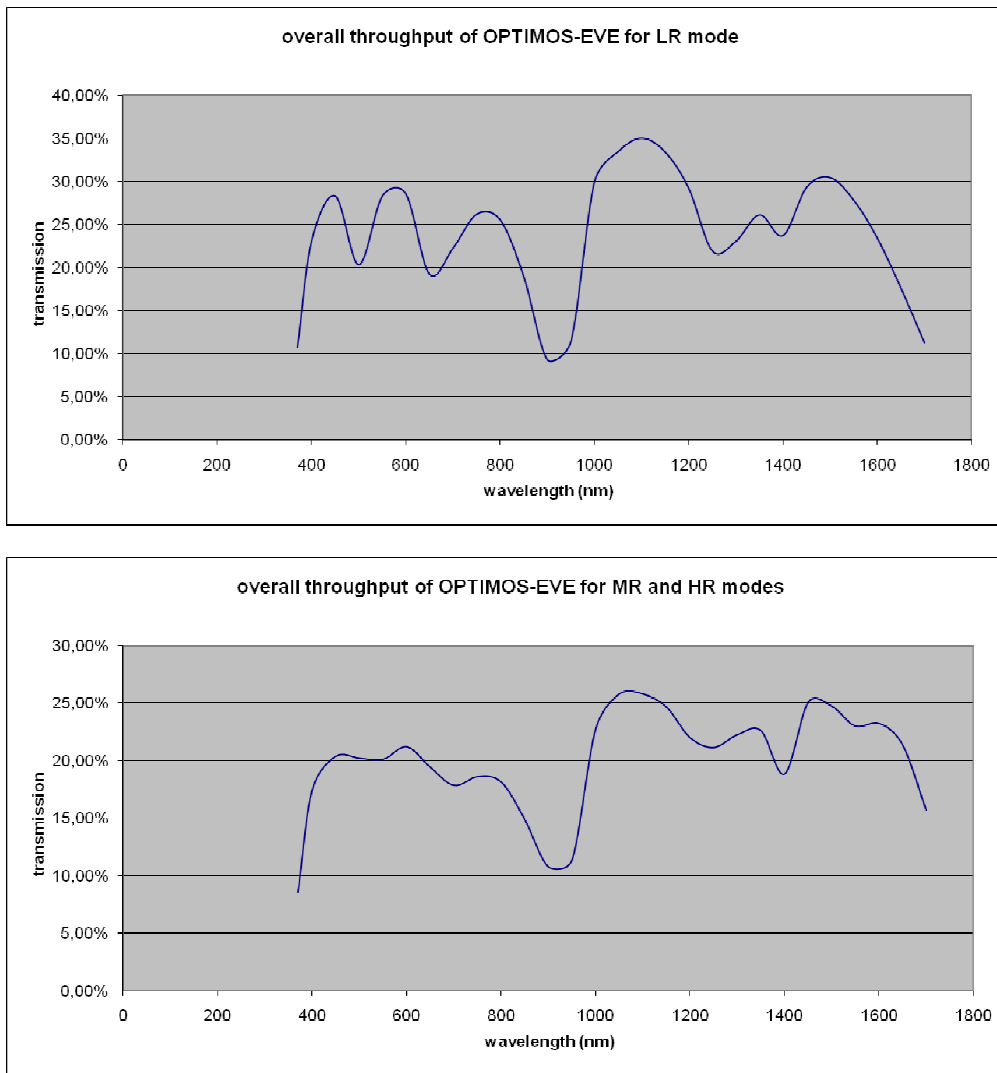


Figure 10. Expected efficiency curves at different observing modes, including all light losses from the telescope focal plane to the detector focal plane (QE included).

4. CONCLUSIONS

After comparing many different classes of solution for medium-to-high resolution spectrograph with large multiplexing factors, high-efficiency over a wide bandwidth spanning from the near UV to the H-band, we identified a relatively simple solution, based onto existing state-of-the-art technologies.

All scientific and technical requirements were successfully met. Dispersion is done through large optimized VPH gratings, as large as present day manufacturing technologies, or available within reasonable amount of time and cost. Collimator and camera optics have been designed to fully match parameters of those dispersers, in order to fully exploit their characteristics. Wherever possible a limited amount of aspherical surfaces have been used, to make them feasible with current polishing techniques.

ACKNOWLEDGEMENTS

First and foremost, we would like to thank the entire OPTIMOS-EVE scientific and technical team for their hard work and invaluable contributions to the success of this phase A study. Looking forward we thank all of those who support the OPTIMOS-EVE project in any respect during the completion of the E-ELT.

REFERENCES

- [1] Chemla, F., Dalton, G., Guinouard, I., Pragt, J., Sawyer, E., Spanò, P., Tosh, I.A., Andersen, M., Navarro, R., Hammer, F., Kaper, L., "OPTIMOS-EVE design trade-off analysis," *this Proceeding*, (2010)
- [2] Guinouard, I., Chemla, F., Huet, J., Hammer, J., Flores, H., "Development of five multifibre links for the OPTIMOS-EVE study for the E-ELT," *Proc. SPIE 7739*, (2010)
- [3] http://www.schott.com/advanced_optics/english/download/schott_calcium_fluoride_2010_en.pdf
- [4] Blanche, P.A., Habraken, S.L., Lemaire, P.C., Jamar, C.A.J., "Large-scale DCG transmission holographic gratings for astronomy," *Proc. SPIE 4842*, 31 (2003)
- [5] Blanche, P.A., Gailly, P., Habraken, S.L., Lemaire, P.C., Jamar, C.A.J., "Mosaiced and high line frequency VPH gratings for astronomy," *Proc. SPIE 5494*, 208 (2004)
- [6] Dalton, G., B., Whalley, M., Sawyer, E., Tosh, I., Terrett, D., "Fibre positioning revisited: the use of an off-the-shelf assembly robot for OPTIMOS-EVE," *Proc. SPIE 7739*, (2010)